Electric Field Effects on Photoluminescence of Polyfluorene Thin Films: Dependence on Excitation Wavelength, Field Strength, and Temperature†

Mohan Singh Mehata,‡,|| Chain-Shu Hsu,§ Yuan-Pern Lee,§ and Nobuhiro Ohta*,‡

Research Institute for Electronic Science (RIES), Hokkaido University, Sapporo 001-0020, Japan, and Department of Applied Chemistry, National Chiao Tung University, Hsinchu 30010, Taiwan

Received: March 15, 2009; Revised Manuscript Received: April 23, 2009

Electroabsorption (E-A) and electrophotoluminescence (E-F) spectra of thin films of blue-light-emitting poly(9,9-dioctylfluorene) (PFO) have been measured at temperatures ranging from 25 to 295 K to examine both the optical property and excitation dynamics of these films in the presence of external electric fields of 0−1.2 MV cm^{-1}. Electric field effects on excitation dynamics depend on not only applied field strength but also excitation wavelength and temperature. For photoexcitation at 344 or 402 nm, E-F spectra observed with low applied fields show only the Stark shift, whereas fluorescence quenching is induced only by strong electric fields. For photoexcitation at a shorter wavelength of 298 nm, on the other hand, field-induced quenching of fluorescence is observed even with a weak electric field at any temperature. The presence of a nonradiative process from highly excited states that is effectively affected by electric fields is suggested.

1. Introduction

Conjugated polymers are commonly used for the energy conversion between light and electric power, and diverse applications are possible in devices such as organic light-emitting diodes (OLEDs), field-effect transistors, solar cells, or laser materials.[1−3] With organic polymers combined with the spin coating technique or inkjet printing method, preparations of low-cost electronic devices and large-size devices are possible, in contrast with devices prepared from small molecules combined with the vapor deposition technique.[3,4]

Physical properties of polymer materials have been extensively examined using various optical methods including time-resolved fluorescence spectroscopy, ultrafast pump−probe spectroscopy, scanning near-field optical microscopy, etc. to understand the excited-state dynamics and photofunctionality of the materials.[5−7] To design and develop more efficient and more stable organic devices, an enhanced understanding of the excitation dynamics of materials is essential. Furthermore, to understand the intrinsic properties of a device configuration, e.g., in OLEDs or in solar cells, it is indispensable to study the excitation dynamics of polymers under the influence of an external electric field following optical excitation. In some conjugated polymers, electroabsorption measurements were performed, and the symmetry breaking in the polymer film and the Stark shift in the spectra of the polymer films has been discussed.[8] As far as the excited-state dynamics in the presence of strong electric fields is concerned, however, experimental research has been unreported so far.

Poly(9,9-dioctylfluorene), i.e., polyfluorene (PFO), has emerged as an especially attractive conjugated polymer due to its strong blue light emission (blue OLEDs) and excellent electronic properties, which bears a large extinction coefficient, high fluorescence quantum yield, and high hole mobility, that show great prospect for device application.[9−12] Such applications rely on injection and transport of charge carriers.[13] The photophysical properties of PFO are known to vary strongly with the morphology of the thin film.[14−16] The elucidation of the emissive species of PFO has been an active area of research due to the complexity of the emission spectrum and the apparent sensitivity to processing conditions.[17−23]

In the present study, external electric field effects on the optical spectra of PFO thin films have been examined. Electric field-induced changes in absorption and photoluminescence spectra as a function of wavelength or wavenumber, i.e., the so-called electroabsorption (E-A) and electrophotoluminescence (E-F) spectra, respectively, were obtained using electric field modulation spectroscopy at different field strengths, different excitation wavelengths, and different temperatures. Direct measurements of the electric-field-induced change in fluorescence decay profile have been also carried out at different external field strengths at different excitation wavelengths. Besides the Stark shift resulting from the change in electric property between the ground state and emitting state, electric-field-induced change in excitation dynamics is observed, which depends on the excitation wavelength. Based on the experimental results of both the E-F spectra and the field-induced change in decay profile, the mechanism of the field-induced quenching of fluorescence is discussed.

2. Experimental Section

PFO was synthesized via a palladium-catalyzed Suzuki coupling reaction of 2,7-bis-1,3,2-dioxaborolanyl-9,9-dioctylfluorene and 2,7-dibromo-9,9- dioctylfluorene.[1,24,25] The average molecular weight was 113 166, and the polydispersity was 2.32. The PFO film was deposited on an indium-tin-oxide (ITO) coated quartz substrate by a spin coating method from toluene solution, and then poly(methyl methacrylate) (PMMA) film was deposited on the PFO film. A semitransparent aluminum film (Al) was further deposited on the PMMA film by a vacuum vapor deposition technique. ITO and Al were used as electrodes

† Part of the "Hiroshi Masuhara Festschrift".

* To whom correspondence should be addressed. E-mail: nohta@es.hokudai.ac.jp.

‡ Hokkaido University.

§ National Chiao Tung University.

|| Permanent Address: Photophysics Laboratory, Department of Physics, DSB Campus, Kumaun University, Nainitial 263 002, Uttarakhand, India.

10.1021/jp9023052 CCC: $40.75 © 2009 American Chemical Society
Published on Web 05/14/2009

in the E-A and E-F measurements. The thickness of the PFO film was determined to be 20−50 nm, based on the UV−visible absorption intensity of the sample and the relation between optical density and the thickness of the PFO film given in the literature.[26] The thickness of PMMA films, typically 0.5 μm, was measured with an interferometric microscope (Nano Spec/AFT 010−0180, Nanomatric). E-A and E-F spectra were obtained at the second harmonics of the modulation frequency of the applied electric field. Hereafter, applied electric field is denoted by **F**, and its strength is represented by the rms value.

Absorption measurements were performed with a Hitachi U-3500 spectrophotometer. Polarized E-A spectra were measured at the normal angle and at the magic angle between the direction of **F** and the electric vector of the excitation light under atmospheric conditions with the same apparatus as described elsewhere.[27] A convergent light beam from the Xenon lamp of Jasco FP-777 spectrofluorometer, i.e., excitation light dispersed by the monochromator installed in the spectrofluorometer was collimated and directed through an α-barium borate polarization prism (CASIX, JDSU) and through the sample slide to an external photomultiplier, which was further amplified and divided into two channels. The dc component was directly collected with a computer, and the ac component synchronized with the applied voltage was recorded with a lock-in amplifier (SR830, SRS). The amplitude and the phase signals from the output of the lock-in amplifier at the second harmonics of the modulation frequency ($\Delta I(2\nu)$) were digitized and recorded, together with the dc component of the transmitted excitation light intensity. The change in absorption intensity, i.e., ΔA, caused by the applied electric field is defined as $\Delta A = -(2\sqrt{2}/\ln 10)\Delta I(2\nu)/I$, where the factor $2\sqrt{2}$ converts the value of measured rms signal to it is equivalent dc signal, and I and ΔI represent the transmitted light intensity and its field-induced change, respectively.

E-F spectra were measured under vacuum conditions at temperatures in the range of 25−295 K.[28] The sample substrate was cooled using a cryogenic refrigerating system (Daikin, V202C5LR) equipped with quartz optical windows, and the temperature of the substrate was controlled and monitored using a temperature controller (Scientific Inst., model 9600) with a silicon diode thermometer (Scientific Int., Si410A). The photoluminescence intensity at zero field and its field-induced change are represented by I_F and ΔI_F ($=I_{F(F\neq 0)} - I_{F(F=0)}$), respectively. It is noted that E-F spectra are different from the so-called electroluminescence (EL) spectra; E-F spectra are obtained as a result of the electric-field-induced change in photoluminescence (PL) spectra, while EL spectra are obtained in the presence of electric fields without photoirradiation. In the present measurements of the E-F spectra, the contribution of the EL intensity was negligible; an insulator film of PMMA was inserted between PFO film and Al electrode. In every case, E-F spectra were obtained with excitation at wavelengths at which the field-induced-change in absorption intensity was negligible. The observed change in total emission intensity in the presence of **F** is therefore ascribed to the field-induced change in the total emission quantum yield, which might result from the field-induced change in the population of the emitting state and/or the quantum yield of the emitting state.

Fluorescence decays were measured with a time-correlated single-photon counting (TCSPC) fluorescence lifetime measurement system, using a mode-locked Ti:sapphire laser (Spectra Physics, Tsunami) as an excitation light source.[29] The second and third harmonics of the laser light generated with an ultrafast harmonic system (Inrad, model 5−050), whose pulse width was ~200 fs, were used as an excitation light. The repetition rate of the excitation laser light was reduced from 80 to 6.8 MHz using an E. O. modulator (Conoptics, model 350−160). Fluorescence from the sample was dispersed with a monochromator (Nikon, G-250) and detected with a microchannel-plate photomultiplier (Hamamatsu, R3809U-52). The fluorescence signal was amplified, discriminated, and then fed to a time-to-amplitude converter (TAC) system as a start pulse. Fluorescence decays were obtained with a multichannel pulse-height analyzer (SEIKO EG&G, 7700). The instrumental response function had a pulse width of ~60 ps (fwhm).

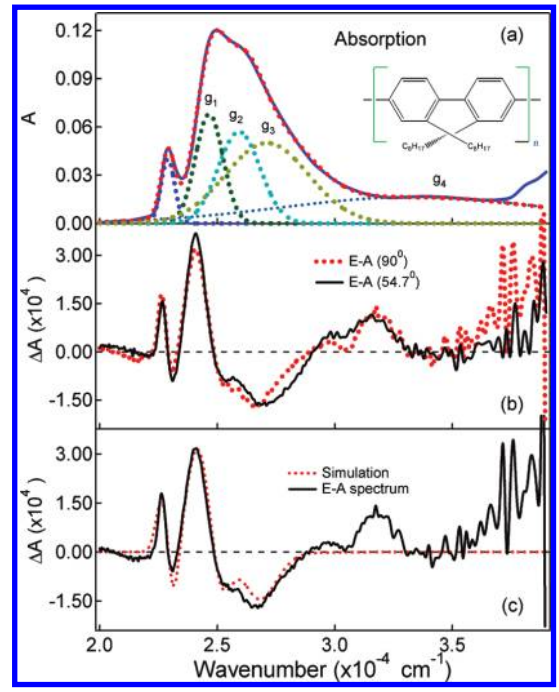

Figure 1. (a) Absorption spectrum of PFO film, (b) electroabsorption (E-A) spectra of PFO film observed at two different angles of χ (= 90° and 54.7°) with a field strength of 0.7 MVcm^{-1}, (c) simulated E-A spectrum, together with the observed one with χ = 90°. Thick dotted line in (a) shows the spectrum simulated by a sum of the β-band and g_1-g_4 bands, each of which is given by a dotted line.

In the measurements of the electric-field-induced change in the decay profile, modulated voltage was applied to samples.[29] A TCSPC system was combined with a pulse generator supplying a bipolar square wave. The applied voltage has a repetition of rectangular waves of positive, zero, negative, and zero bias in turn, with a duration of 30 ms for each bias. We start data acquisition 2 ms after each bias step to exclude an overshooting effect of applied field just after the change in applied voltage. The memory channel of the multichannel pulse height analyzer (MCA) was divided into four segments. A switching of MCA is synchronized with a modulated applied voltage. Four different decays were collected, corresponding to positive, zero, negative and zero sample biases, respectively. These decays were stored in separate memory segments of MCA.

3. Results and Discussion

3.1. Electric Field Effect on Absorption Spectra. Polarized E-A spectra and absorption spectra of the PFO film were observed at a field strength of 0.7 MVcm^{-1}. The results are shown in Figure 1. PFO thin films have two distinct conformational phases, the glassy phase (g-phase) and the more ordered β-phase,[23,26,30−39] as well as highly localized oxidative

CHART 1: Chemical Structure of Fully Extended Segment of PFO (Planar Phase)

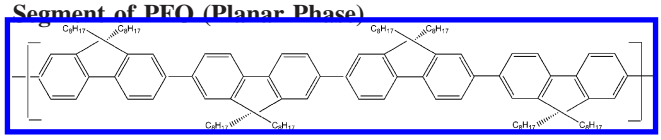

emissive defects[36,37] which in turn depend on the alkyl side groups. The observed absorption spectrum in Figure 1a, which is similar to those reported previously,[23,26] shows a strong band with a peak at ~400 nm (~25 000 cm^{-1}) and a sharp band with a peak at 436 nm (~23 000 cm^{-1}). The 400-nm band is ascribed to the g-phase of PFO, i.e., disordered phases of PFO, whereas the band at 436 nm is assigned to the so-called β-phase.[23] In the β-phase, the octyl side chains arrange in an antigauche−gauche conformation or 2_1 helix (see chemical structure shown in Chart 1), which is energetically favored, and an individual polymer chain can adopt a longer conjugation length, hence exhibit a red-shifted absorption relative to the disordered phase.[21,40] The percentage of the polymer chains forming the β-phase relative to the g-phase depends strongly on the polarity of the solvent from which the PFO was cast from or to which it was subsequently exposed, and is reported to be in the region of 8−50%.[20,21,26] Deposition of a PMMA layer on the PFO film increases the percentage of the β-phase, similar to the sample exposed to toluene vapor.[31]

Polarized E-A spectra were obtained with the incident angle normal to the surface ($\chi = 90°$) and with the magic angle ($\chi = 54.7°$) under atmospheric conditions. Here, χ is the angle between the direction of applied electric field and the electric vector of the incident light. As shown in Figure 1, both spectra are nearly the same, indicating an isotropic distribution of PFO and the immobility of PFO films in the presence of **F**. The magnitude of the change in absorption intensity (ΔA) was confirmed to be proportional to the square of the applied field strength.

By assuming the isotropic distribution of the PFO films, the field-induced change in absorption intensity (E-A spectrum) at frequency, ν, observed at the second harmonics of the modulation frequency may be given by the following equation:[41−44]

$$\Delta A(\nu) = (fF)^2\left[A_\chi A(\nu) + B_\chi \nu \frac{\mathrm{d}}{\mathrm{d}\nu}\left\{\frac{A(\nu)}{\nu}\right\} + C_\chi \nu \frac{\mathrm{d}^2}{\mathrm{d}\nu^2}\left\{\frac{A(\nu)}{\nu}\right\}\right] \quad (1)$$

The coefficient A_χ corresponds to the field-induced change in absorption intensity. The coefficients B_χ and C_χ correspond to the spectral shift and spectral broadening of the absorption spectra resulting from the change in molecular polarizabilty ($\Delta\alpha$) and in electric dipole moment ($\Delta\mu$), respectively, following the optical transition. These coefficients are expressed as

$$B_\chi = \frac{\Delta\bar{\alpha}}{2hc} + \left\{\frac{(\Delta\alpha_m - \Delta\bar{\alpha})(3\cos^2\chi - 1)}{10hc}\right\} \quad (2)$$

$$C_\chi = |\Delta\mu|^2\left\{\frac{5 + (3\cos^2\chi - 1)(3\cos^2\eta - 1)}{30h^2c^2}\right\} \quad (3)$$

where $|\Delta\mu| = |\mu_e - \mu_g|$ and $\Delta\bar{\alpha} = {}^1/_3\mathrm{Tr}(\Delta\alpha)$; subscripts e and g represent the excited and ground states, respectively. In these equations, h represents Planck's constant and c is the speed of light. $\Delta\alpha_m$ represents the diagonal component of $\Delta\bar{\alpha}$ with respect to the direction of the transition dipole moment, and η is the angle between the direction of $\Delta\boldsymbol{\mu}$ and the transition dipole moment.

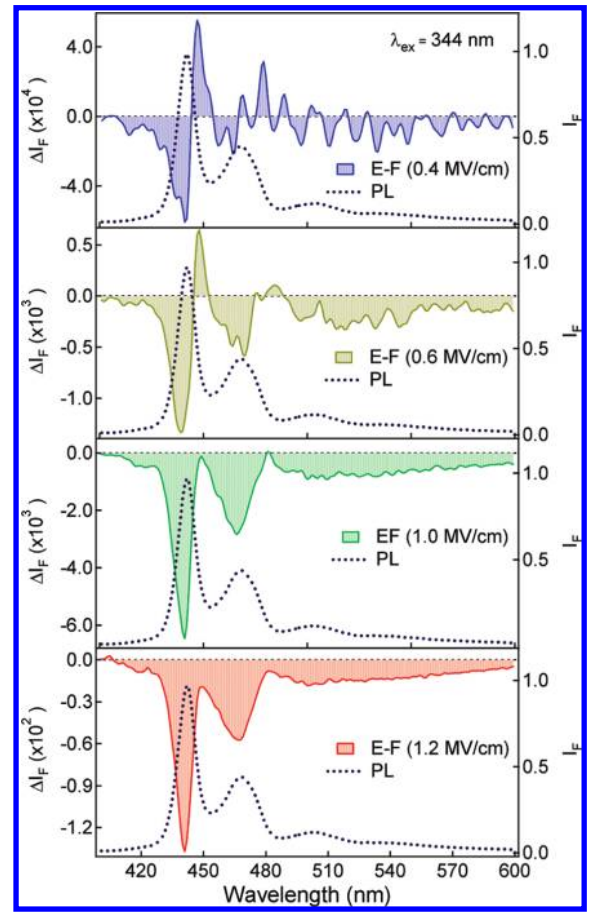

Figure 2. E-F spectra as well as PL spectra of PFO film obtained with 344-nm excitation at different field strengths in the region of 0.4 − 1.2 MV cm^{-1}. The maximum PL intensity is normalized to unity in every case.

As shown in Figure 1, the E-A spectra at wavenumbers less than 30 000 cm^{-1} could be reproduced by the first-derivative spectra of both g- and β-forms of PFO. Actually, the g-phase absorption was reproduced by a superposition of four Gaussian bands, g_1−g_3 bands, which likely correspond to three different states,[8,15] and another Gaussian band g_4 (see Figure 1). The first derivatives of the three g-phase Gaussian bands and the β-phase band were used to simulate the E-A spectra, and the change in molecular polarizability ($\Delta\bar{\alpha}$) following the optical transition from the ground state to the excited state were determined to be 263, 270, and 7 $Å^3/f^2$ for the g_1−g_3 bands, respectively, and 132 $Å^3/f^2$ for the β-phase, assuming that the molecular polarizability is isotropic, i.e., $\Delta\alpha_m = \Delta\bar{\alpha}$ in eq 2. Here, f is the internal field factor. These values are 1 order of magnitude smaller than those reported previously.[8,14] The g_4 band was excluded in the simulation and we made no attempt to reproduce the E-A spectra at wavenumbers above 30 000 cm^{-1}.

3.2. Electric Field Effects on Photoluminescence and Excitation Dynamics. E-F and PL spectra of PFO films were obtained at room temperature under vacuum condition at applied field strengths of 0−1.2 MV cm^{-1}. Excitation was performed at the wavelengths at which the field-induced change in absorption intensity was negligible, e.g., 298 and 344 nm, and E-F and PL spectra were obtained simultaneously. The results with excitation at 344 and 298 nm are shown in Figures 2 and 3, respectively. According to the absorption spectrum in Figure

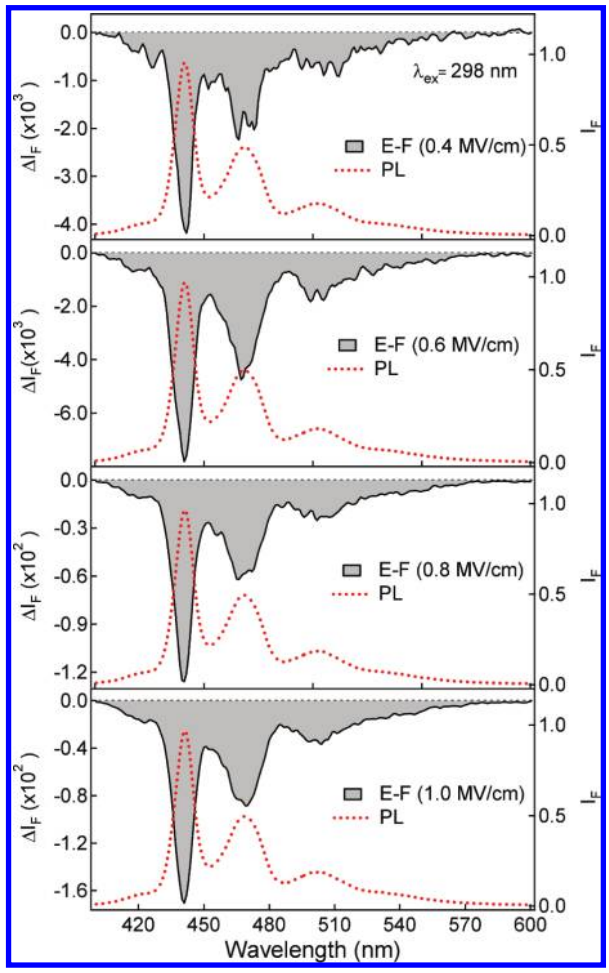

Figure 3. E-F spectra as well as PL spectra of PFO film obtained with 298-nm excitation at various field strengths in the region of 0.4 − 1.0 MV cm^{-1}. The maximum PL intensity is normalized to unity in every case.

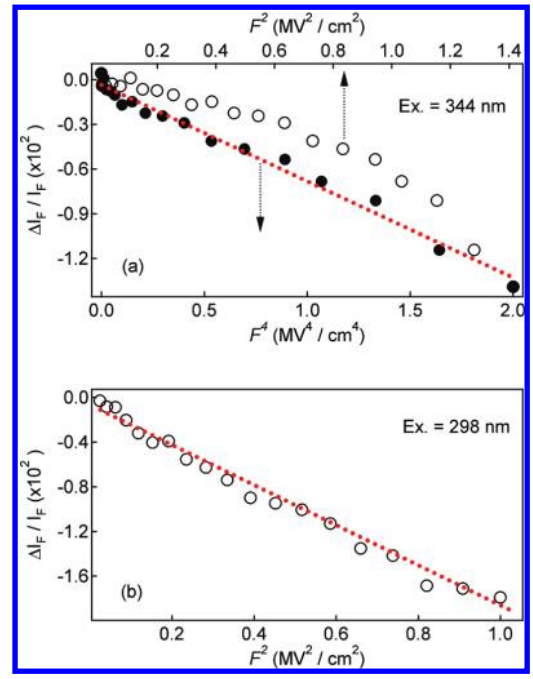

Figure 4. Plots of $\Delta I_F/I_F$ as a function of square of the applied field strength with 344-nm excitation (a) and with 298-nm excitation (b). Plots of $\Delta I_F/I_F$ as a function of the fourth power of the applied field strength are also shown in (a) for the 344-nm excitation. Dotted straight line is just a guide for eye.

1, PFO films are composed of mainly the g-phase, with a small fraction of the β-phase. Fluorescence of PFO films in the g-phase is located in the shorter wavelength region than that of the β-phase.[23] As shown in Figure 2, PL spectra (dotted lines) show a strong band at 441 nm, irrespective of excitation wavelength. This band and associated vibronic bands at 469, 504, and 540 nm are assigned to the fluorescence emitted from the β-phase of PFO.[34] The fact that β-phase emission is dominant indicates that efficient excitation energy transfer occurs from g-phase to β-phase.[19] This effect is expected as there is a strong overlap between the emission spectrum of the g-phase and the absorption spectrum of the β-phase, which allows an efficient energy transfer according to Förster-type mechanisms, if they are sufficiently well intermixed. In fact, it is reported that the relaxation dynamics of PFO involves efficient energy transfer within or between two phases.[26,38,39]

With excitation at 344 nm, the E-F spectrum observed with a field strength of 0.4 $MVcm^{-1}$ shows the shape of the first derivative of the PL spectrum (see Figure 2, shaded line), indicating that only the Stark shift resulting from the difference in molecular polarizability between the emitting state and the ground state appears when the applied field is not so strong. Note that the field-induced change in PL spectrum, i.e., E-F spectrum, is given by an equation similar to eq 1,[43] that is, by a linear combination between the zeroth, first, and second derivatives of the PL spectrum, and the first and second derivatives come from the difference in molecular polarizability and electric dipole moment, respectively, between the emitting state and the ground state. The result that the E-F spectrum is essentially the same as the first derivative of the emission spectrum indicates that the fluorescence quantum yield is not affected by **F** at 344-nm excitation, when the applied field strength is not so strong. As the applied field increases, however, the shape of the E-F spectrum becomes similar to the one of the PL spectrum, as shown in Figure 2. The integrated intensity of the E-F spectrum becomes negative, indicating that the emission quantum yield becomes smaller in the presence of **F**; fluorescence of FPO thin films is quenched by application of strong electric fields at 344-nm excitation. The field strength dependence of ΔI_F was obtained by integrating the E-F spectra. The results are shown in Figure 4, in which plots of ΔI_F are presented as a function of the square of the applied field strength or as a function of the fourth power of the applied field strength. It is worth mentioning that $\Delta I_F/I_F$ may correspond to the field-induced change in nonradiative decay rate relative to the total decay rate at the emitting state. As shown in Figure 4, the magnitude of the quenching, i.e., ΔI_F, is proportional to the fourth power of **F**, rather than to the square of **F**. With excitation at wavelengths longer than 344 nm, e.g., at 402 nm, similar results were obtained, as shown in Figure 5. With 402-nm excitation, E-F spectra obtained with a field of 0.4 or 0.6 MV cm^{-1} show the shape given by the first derivative of the PL spectra, indicating that only the Stark shift resulting from the difference in molecular polarizability between the emitting state and the ground state appears, as the electric field effect. As the applied field increases, the observed E-F spectra are given by a linear combination between the zeroth and first derivative spectra of the PL spectra. Thus, fluorescence of PFO shows not only the Stark shift but also the field-induced quenching with strong fields. The field strength dependence of fluorescence intensity observed at 402-nm excitation is similar to the one at 344-nm excitation.

The magnitude of the Stark shift observed in the present study for the randomly distributed PFO films is proportional to the

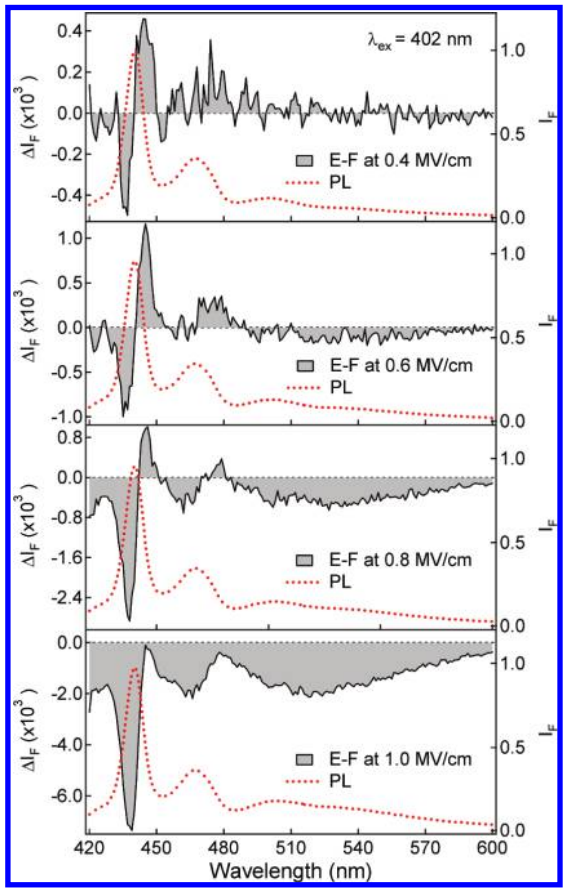

Figure 5. E-F spectra of PFO film obtained with excitation at 402 nm at various field strengths of 0.4−1.0 MV cm^{-1}, together with the PL spectra. The maximum PL intensity is normalized to unity in every case.

square of the applied field strength, and the Stark shift of PFO is regarded as caused by the difference in molecular polarizability between the emitting state and the ground state of PFO films, as mentioned above. The present result of PFO films is very different from the Stark shift observed for conjugated polymers of poly(2-methoxy-5-(2′-ethyl-hexyloxy)-1,4-phenylene-vinylene (MEH-PPV) or methyl-substituted ladder-type poly(*p*-phenylene) (LPPP). Lupton and co-workers reported that electric field applied in low temperature single molecule spectroscopy of MEH-PPV or LPPP showed linear Stark shifts in the emission of single chromophores on individual chains of MEH-PPV or LPPP.[5] Thus, the observed Stark shift of MEH-PPV or LPPP is caused by the difference in electric dipole moment between the emitting state and the ground state, and the Stark shift caused by the difference in molecular polarizability between the emitting state and the ground state, which is important in PFO films, was not referred for MEH-PPV and LPPP.

With excitation at shorter wavelengths, e.g., at 298 nm, electric field effects on PL spectra of PFO films are very different from those with excitation at longer wavelengths such as 344 or 402 nm, and fluorescence of PFO films is quenched by **F** even when the applied field is as low as 0.4 MV cm^{-1} (see Figure 3). As shown in Figure 4, the magnitude of the fluorescence quenching monotonically increases with increasing field strength. Actually, ΔI_F at 298-nm excitation is proportional to the square of **F**, in contrast to the results of excitation into lower excited states. These results imply that the mechanism of field-induced quenching upon excitation into higher excited states is different from that observed upon excitation into low-lying excited states at strong applied fields. Thus, the field-induced quenching of the PFO fluorescence depends strongly not only on the applied field strength but also on the excitation wavelength.

E-F spectra as well as PL spectra were also obtained at different temperatures. The results at 295 and 40 K with excitation at 344 nm are shown in Figure 6. As the temperature decreased, emission bands were slightly red-shifted, and the spectral width became narrower. As the temperature decreased further, PL intensity increased monotonically (see Figure 7), indicating that the rate of the nonradiative process at the emitting state of PFO films becomes smaller, as the temperature decreases. Lowering the temperature has two effects; the increase of the dielectric constant due to the densification and the increased conjugate length due to improved ordering of the polymer backbone.[23] As pointed out for poly(phenylenevinylene), the decrease in bandwidth at low temperatures might result from the freezing out of the librational and rotational modes at low temperatures, and the red-shift of the band might be correlated with the increased conjugated length at low tempeartures.[38]

At 344-nm excitation, the E-F spectra at 295 K observed at high fields are similar in shape to the PL spectra (zeroth derivative of the PL spectra), whereas the E-F spectra at 40 K are similar in shape to the first derivative of the PL spectra even at high fields, as shown in Figure 6. Actually, the observed E-F spectra at any temperature could be reproduced as a linear combination of the zeroth and the first derivatives of the PL spectrum, as shown in Figure 6. The value of $\Delta\bar{\alpha}$ at 295 K is thereby determined to be 134 $Å^3/f^2$, based on an equation similar to eq 2. It is noted that this value of $\Delta\bar{\alpha}$ is nearly the same as that obtained from the E-A spectrum of the β-phase at room temperature.

As the temperature decreases, the field-induced quenching at 344-nm excitation becomes smaller (see Figure 7), resulting in the increase of the first derivative component relative to the zeroth derivative. For this reason the E-F spectra at low temperatures are similar in shape to the first derivative of the PL spectra. At 40 K, $\Delta\bar{\alpha} = 104$ $Å^3/f^2$, which is smaller than the value at room temperature. The absolute value of the integrated intensity of the E-F spectra, which corresponds to the magnitude of the field-induced quenching of fluorescence, becomes smaller not only with 344-nm but also with 402-nm excitation, as the temperature decreases. Note that the spectral shift given by the first derivative of the spectra has no influence on the integrated intensity. Actually, the magnitude of $|\Delta I_F/I_F|$ suddenly decreases as the temperature decreases from 295 to 240 K, but remains nearly constant at temperatures lower than 240 K at both excitation wavelengths (see Figure 7).

With excitation at 298 nm, the shape of the E-F spectra is nearly the same as that of the PL spectra at any temperature, irrespective of applied field strength (see Figure 8), indicating that fluorescence quenching is the dominant electric field effect at any temperature, independent of field strength. It is worth mentioning that the magnitude of the quenching at longer wavelength excitation observed at strong fields is still much smaller than that with 298-nm excitation. As shown in Figure 7, the magnitude of the field-induced quenching observed with 298-nm excitation decreases slightly as the temperature decreases from 295 to 220 K, which is similar to the temperature dependence at 344-nm or 402-nm excitation. As the temperature further decreases from 220 to 40 K, however, the magnitude of quenching increases, in contrast to the behavior with excitation at 344 or 402 nm (see Figure 7). Thus, the temperature dependence of the field-induced quenching with excitation at

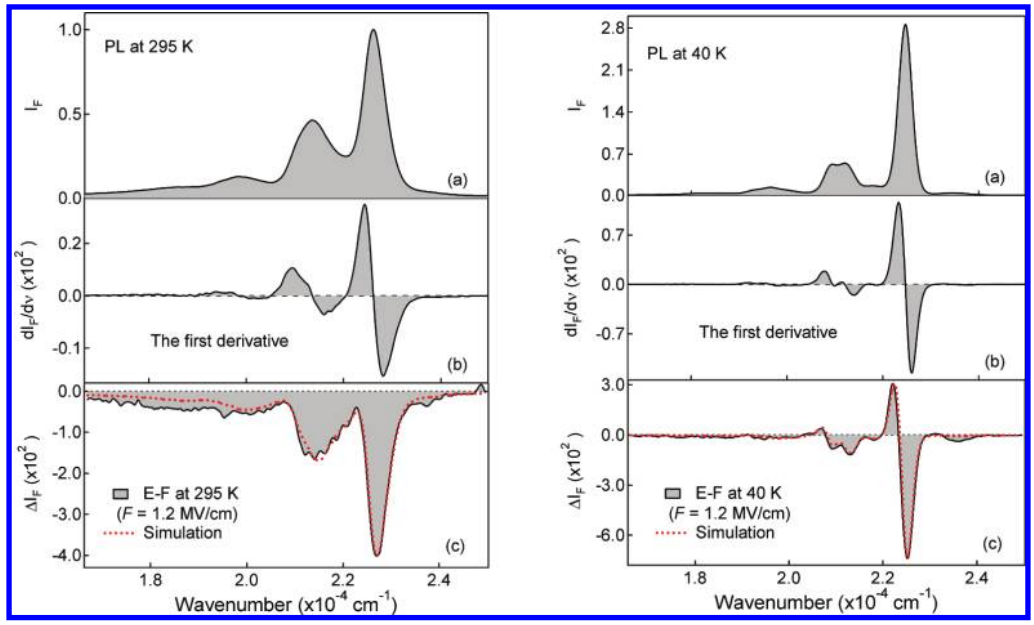

Figure 6. (a) PL spectra of PFO film, (b) the first derivative of PL, (c) E-F spectrum (shaded line) and simulated spectrum (dotted line). The spectra were obtained at 295 K (left) and at 40 K (right) with a field strength of 1.2 MV cm^{-1}. Excitation wavelength was 344 nm. The maximum PL intensity at 295 K is normalized to unity.

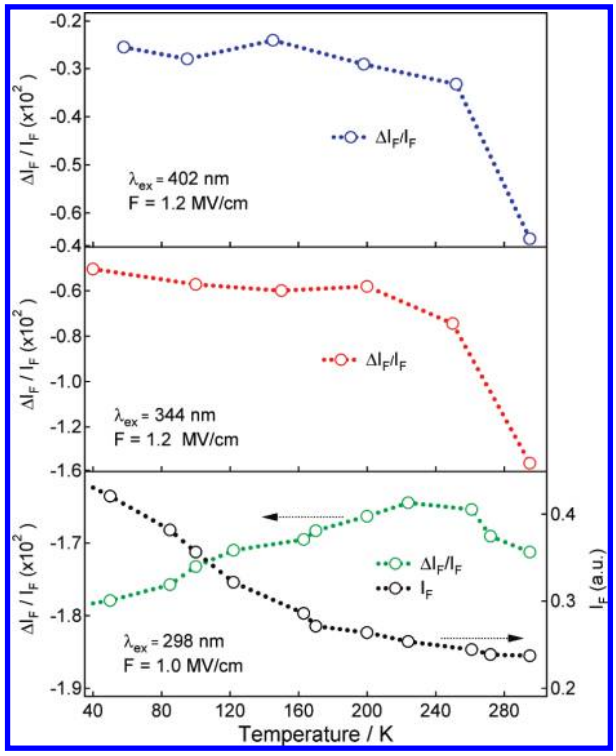

Figure 7. Plots of $\Delta I_F/I_F$ of PFO film as a function of temperature with excitation at 402 nm, 344 and 298 nm. The applied field strength was 1.2 MVcm^{-1} for the 402 and 344 nm excitation. At 298-nm excitation, $\Delta I_F/I_F$ was obtained at 1.0 MVcm^{-1}. Plots of the PL intensity as a function of temperature obtained with 298-nm excitation are also shown in the figure.

298 nm is also different from the one with excitation at 344 or 402 nm, which also supports the presence of different mechanisms for the electric-field-induced quenching of fluorescence of a PFO film.

From only the steady-state emission measurements, it is difficult to confirm whether the field-induced quenching of fluorescence results from an increased nonradiative decay rate at the emitting state, which leads to the decrease in fluorescence quantum yield as well as in fluorescence lifetime, or from a decreased initial population of the emitting species. Then, direct measurements of the field-induced change in fluorescence decay profiles of PFO films were carried out at two different excitation wavelengths, i.e., 298 and 402 nm, at which the field-induced change in absorption intensity was negligible. In both cases, fluorescence was monitored at a peak of the emission band of the β-phase, i.e., at 441 nm.

Figure 9 shows the emission decay profiles of a PFO film measured at 298-nm excitation. The difference, $I_F(t) - I_0(t)$ ($\equiv \Delta I_F(t)$), and the ratio, $I_F(t)/I_0(t)$, between the decay profiles at zero field ($I_0(t)$) and in the presence of **F** ($I_F(t)$) at 0.6 and 1.0 MV cm^{-1} are also shown in Figure 9. It is noted that the initial population of the emitting state of the PFO fluorescence is unaffected by **F**, if the ratio of $I_F(t)/I_0(t)$ is unity at $t = 0$, i.e., just after photoexcitation. If the fluorescence lifetime is independent of **F**, further, $I_F(t)/I_0(t)$ is expected to remain constant over the entire time domain. As shown in Figure 9, $\Delta I_F(t)$ is negative in the entire time domain following photoexcitation, indicating that PFO fluorescence is quenched by **F** at any time range following excitation, in agreement with the steady-state E-F spectra. The fluorescence shows a nearly single exponential decay, i.e., $A_1 \exp(-t/\tau_1)$ with lifetime τ_1 and pre-exponential factor A_1. A rise component was not observed at any excitation in the present experiments, because the fast energy transfer from the excited state to the emitting state exceeds the present time resolution. $I_0(t)$ and $\Delta I_F(t)$, both of which go to zero with a decay, show a similar shape to each other, implying that the lifetime in the presence of electric fields is very similar to the one at zero field. By simulating all time profiles of $I_0(t)$, $\Delta I_F(t)$, and $I_F(t)/I_0(t)$, the field-induced change in lifetime and pre-exponential factor was evaluated. The lifetime at zero field was determined to be $\tau_1 = 311$ ps, and pre-exponential factor $A_1 = 1.0$ is normalized to unity. The corresponding values in the presence of 0.6 and 1.0 MV cm^{-1} are $\tau_1 = 312$ ps ($A_1 = 0.980$) and $\tau_1 = 312$ ps ($A_1 = 0.949$), respectively. Thus, the pre-exponential factor significantly decreases and the lifetime becomes slightly longer in the presence of **F**. It is necessary to realize that the simulated lifetime may include an experimental

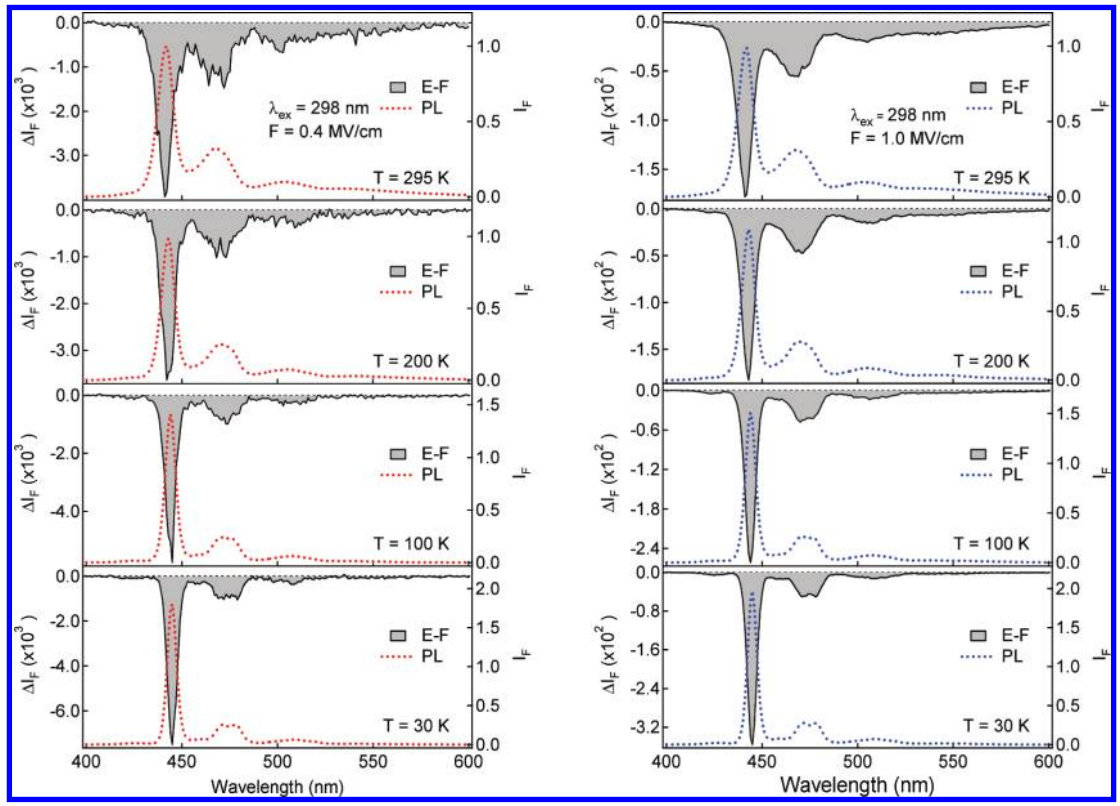

Figure 8. E-F spectra as well as PL spectra obtained at various temperatures with excitation at 298 nm. Applied field strength was 0.4 (left) and 1.0 MV cm^{-1} (right). The maximum PL intensity at 295 K is normalized to unity in both cases.

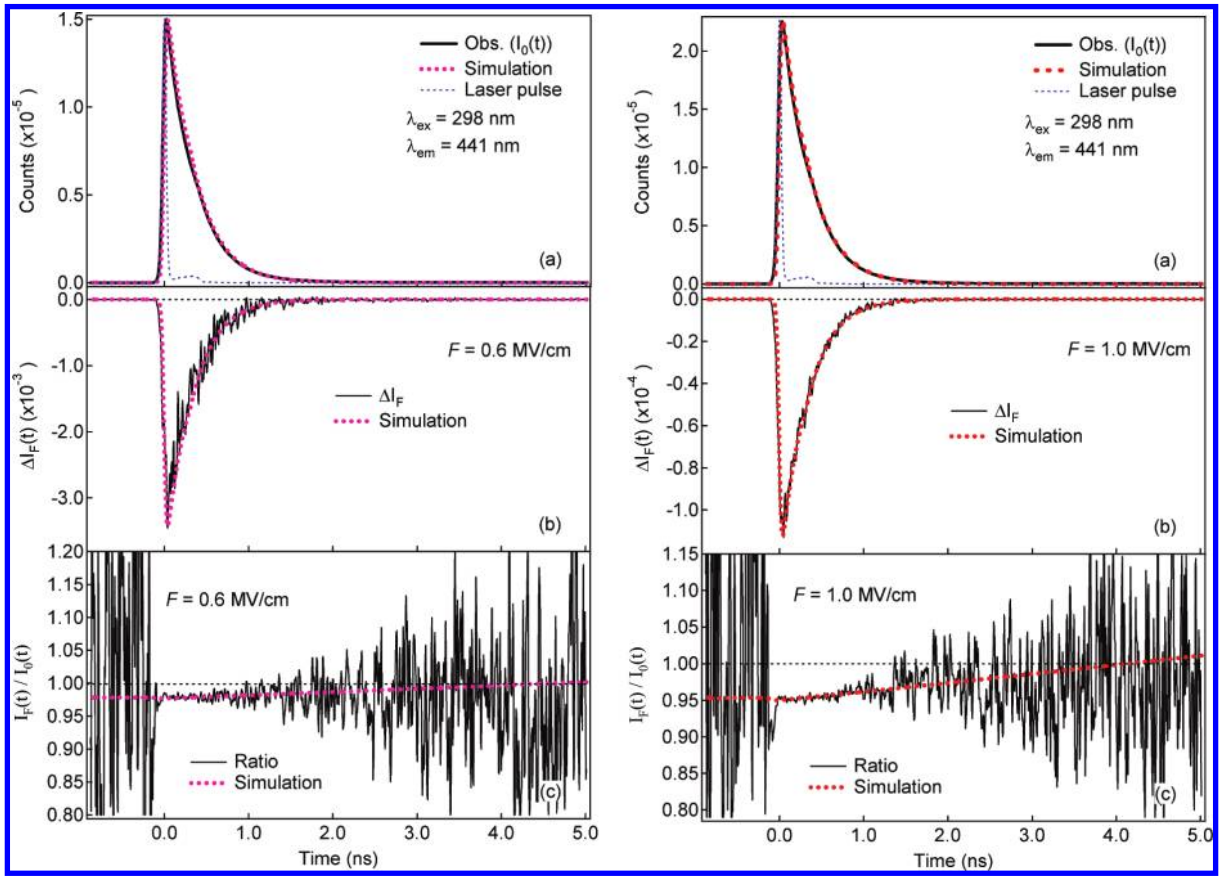

Figure 9. (a) Fluorescence decay (solid line) of PFO film observed at zero field, together with the simulated one (dotted line), (b) difference between the decays observed in the presence of **F** and at zero field, and (c) the ratio of the decay observed in the presence of **F** relative to that at zero field. Applied field strength was 0.6 (left) and 1.0 MV cm^{-1} (right). The instrumental response function is shown in (a) by a thin dotted line. Excitation and emission wavelengths were 298 and 441 nm, respectively.

error of 1∼2%, but the positive slope of $I_F(t)/I_0(t)$, which is clearer at high fields, is consistent with the increased lifetime in the presence of $\boldsymbol{F}$ (see also Figure S1 of the Supporting Information). The fluorescence lifetime at zero field observed in the present experiments is smaller than that reported previously, though the reason is unknown. For example, the decay time was reported for the g- and β-phases of PFO to be 430 ps[19] and the average lifetime of β-phase to be ∼400 ps.[38]

Direct measurements of the decay profile clearly show that the pre-exponential factor is significantly reduced with increasing **F**; the factor decreases by ∼2% at 0.6 MV cm^{-1} and by more than 5% at 1.0 MV cm^{-1}. Then, the field-induced quenching of the PFO fluorescence is attributed to the field-induced decrease in population of the fluorescent PFO just after the photoexcitation. As mentioned above, further, the ratio of $I_F(t)/I_0(t)$ increases slightly with time especially at high fields, indicating that the lifetime of the PFO fluorescence becomes slightly longer in the presence of **F**. The field-induced lengthening of fluorescence lifetime is expected, when the nonradiative decay rate decreases with increasing **F** at the emitting state of the PFO fluorescence. With respect to the increase of the slope of $I_F(t)/I_0(t)$ with time, however, it may be necessary to point out another possibility that delayed fluorescence resulting from a field-induced collision of a hole−electron pair appears with time with strong applied fields.

As mentioned already, when the applied field was very strong, field-induced quenching of fluorescence was observed even with excitation at 402- or 344-nm. With 402-nm excitation and monitoring the emission at 441 nm, the decay profile (I_0(t)), ΔI_F(t) and I_F(t)/I_0(t) were also obtained with an applied field as strong as 1.0 MV cm^{-1}. The results are quite similar to those at 298-nm excitation in the sense that the initial population is reduced with increasing **F** and that the ratio of $I_F(t)/I_0(t)$ increases slightly with time, as shown in the Supporting Information. Actually, the field-induced change of PL intensity at 402-nm excitation is as small as 0.8% even in the presence of 1.0 MV cm^{-1}.

Based on the results of the E-F spectra observed at various excitation wavelengths, field strengths and temperatures, the electric field effects on the photoexcitation dynamics of PFO films clearly depend on both the excitation wavelength and temperature. The excitation energy transfer from g-phase to β-phase following excitation into low lying excited states is unlikely to be influenced by **F**, because only the Stark shift was observed and the emission quantum yield was unaffected by **F** in the presence of 0.4 MV cm^{-1} with excitation at 344 or 402 nm. As the dynamics that is affected by **F**, therefore, physical or chemical processes other than the excitation energy transfer induced by the Förster mechanism must be considered.

As the temperature decreases, the total rate of the nonradiative processes at the emitting state of the PFO film becomes smaller, as known from the temperature dependence of the PL intensity, whereas the intensity monotonically increases. The fact that the emission quantum yield is unaffected by **F** (=0.4 MV cm^{-1}) at 344- or 402-nm excitation indicates that not only the energy transfer from g-phase to β-phase but also the nonradiative processes at the emitting state of PFO films that occur at zero field are unaffected by an application of electric fields. In contrast, the PFO fluorescence is quenched by application of strong electric fields with 344- or 402-nm excitation, which probably suggests that a field-assisted generation of hole−electron pairs followed by charge transport within the same phase or between different phases occurs from the emitting state with strong applied electric fields (mechanism 1). A similar field strength dependence, i.e., the fourth power dependence, was observed for the linked compound of pyrene doped in a polymer film, which was also interpreted in terms of a field-assisted generation of hole and electron pair.[45] This kind of field-assisted process might become less efficient with decreasing temperature.

For excitation into higher excited states, another mechanism which also shows a noticeable electric field effect on the PL intensity has to be considered, as mentioned above. In this mechanism, electric field effect is nearly independent of temperature, in contrast to the above-mentioned mechanism applicable to excitation into lower excited states. If electron transfer occurs within the polymer films from highly excited states of PFO through orbital-overlap such as in the superexchange mechanism, this process might be also affected by application of an electric field because of the field-induced orbital polarization (mechanism 2). Furthermore, the electric field effect on both electron transfer and PL intensity caused by this mechanism seems to be independent of temperature, because the thermal effect is not included in this mechanism. There is no doubt that mechanism 2 works with excitation at 298 nm, but further experiments are necessary for the discussion of the exact threshold of mechanism 2.

By assuming that an optically excited state having sufficient energy autoionizes and results in a formation of a Coulombically bound geminate electron−hole pair, the strong field dependence and the simultaneously weak temperature dependence are expected for the yield of excition dissociation.[46] Upon exciting the sample above the dissociation threshold, the excess energy stored in a vibrationally hot Franck−Condon state may further assist dissociation, resulting in the excitation wavelength dependence of the field-assisted exciton dissociation as well as the field-induced quenching of fluorescence. If the generation of the hole−electron pair directly followed by the field-assisted dissociation is concerned with 298-nm excitation, the field-induced quenching of fluorescence similar to that observed with 344-nm excitation may be expected. As already mentioned, however, the field strength dependence of the quenching with 298-nm excitation is very different from the one with 344-nm excitation (see Figure 4). The fact that the magnitude of the field-induced quenching is proportional to the square of the field strength with 298-nm excitation strongly suggests that the nonradiative decay process itself following photoexcitation, i.e., electron transfer process occurring from highly excited state, is influenced by applied electric fields, as suggested as mechanism 2.

The present results of the dependence on field strength, temperature, and excitation wavelength seem to be pertinent to the mechanism of OLEDs as well as to their high performance. For example, the observed temperature dependence might indicate that the performance of OLED with PFO might be improved on lowing the operation temperature; the emission quantum yield is increased and field-induced quenching is reduced on lowing the temperature to ∼240 K, which seems to be strongly related to the efficiency and stability of the OLED devices.

4. Summary

PL spectra and absorption spectra of thin films of PFO have been examined in the presence of external electric fields in the range of 0−1.2 MV cm^{-1}. The applied electric field induces a spectral shift of both absorption and fluorescence spectra of PFO to yield a line shape represented by the first derivative of absorption and the PL spectra, respectively, indicating that the

molecular polarizability is different between the excited and ground states. With excitation into lower excited states, the fluorescence intensity is unaffected by **F** when the applied field strength is as low as 0.4 MV cm^{-1}, indicating that the energy transfer from these lower excited state to the emitting state of the PFO fluorescence and the relaxation rate of the emitting state are unaffected by **F**. As the applied field becomes stronger, however, the fluorescence of PFO films is quenched by **F** even with excitation into low excited states. This quenching is ascribed to the field-assisted generation of hole−electron pairs followed by efficient charge transport (mechanism 1). With excitation into higher excited states, the fluorescence of PFO is quenched even when the applied field is weak, and the magnitude of the quenching increases with increasing field strength, which is ascribed to the electron transfer from highly excited state through orbital-overlap (mechanism 2). Thus, two mechanisms are considered to exist for the field-induced quenching of PFO fluorescence. The field-induced quenching of fluorescence by mechanism 1 becomes less efficient, as the temperature decreases, whereas the quenching by mechanism 2 seems to be nearly independent of temperature. The direct measurements of the field-induced change in the emission decay profile confirm that fluorescence quenching arises from a decreased initial population of the emitting species in both mechanisms. The present study is strongly related to a quest for high performance of molecular devices, e.g., for the design and development of efficient and stable light-emitting devices.

Acknowledgment. M.S.M. thanks to Japan Society for the Promotion of Science for JSPS Postdoctoral fellowship and for a Grant in Aid for JSPS fellows. This work was also supported by Interchange Association, Japan (Japan-Taiwan Joint Research Program).

Supporting Information Available: Additional figure showing fluorescence decay spectra. This material is available free of charge via the Internet at http://pubs.acs.org.

References and Notes

(1) Bernius, M. T.; Inbasekaran, M.; O'Brien, J.; Wu, W. *Adv. Mater.* **2000**, *12*, 1737.
(2) Grice, A. W.; Bradley, D. D. C.; Bernius, M. T.; Insbasekaran, M.; Wu, W. W.; Woo, E. P. *Appl. Phys. Lett.* **1998**, *73*, 629.
(3) Halls, J. J. M.; Arias, A. C.; MacKenzie, J. D.; Wu, W.; Inbasekaran, M.; Woo, E. P.; Friend, R. H. *Adv. Mater.* **2000**, *12*, 498.
(4) Forrest, S. R. *Nature* **2004**, *428*, 911.
(5) Schindler, F.; Lupton, J. M.; Müller, J.; Feldmann, J.; Scherf, U. *Nat. Mat.* **2006**, *5*, 141, and reference cited therein.
(6) Xu, Q. H.; Moses, D.; Heeger, A. J. *Phys. Rev. B* **2004**, *69*, 113314.
(7) Scheblykin, I. G.; Yartsev, A.; Pullerits, T.; Gulbinas, V.; Sundstrom, V. *J. Chem. Phys. B* **2007**, *111*, 6303.
(8) Tong, M.; Sheng, C. X.; Vardeny, Z. V. *Phys. Rev. B* **2007**, *75*, 125207.
(9) Leclerc, M. *J. Polym. Sci. Polym. Chem. Ed.* **2001**, *39*, 2867.
(10) Redecker, M.; Bradley, D. D. C.; Inbasekaran, M.; Woo, E. P. *Appl. Phys. Lett.* **1999**, *74*, 1400.
(11) Prins, P.; Grozema, F. C.; Nehls, B. S.; Farrell, T.; Scherf, U.; Siebbeles, L. D. A. *Phys. Rev. B* **2006**, *74*, 113203.
(12) Scherf, U.; List, E. J. W. *Adv. Mater.* **2002**, *14*, 477.
(13) Burin, A. L.; Ratner, M. A. *J. Polym. Sci., Part B: Polym. Phys.* **2002**, *41*, 2601.
(14) Cadby, A. J.; Lane, P. A.; Mellor, H.; Martin, S. J.; Grell, M.; Giebeler, C.; Bradley, D. D. C. *Phys. Rev. B* **2000**, *62*, 15604.
(15) Gadermaier, C.; Grasse, F.; Perissinotto, S.; Graf, M.; Galbrecht, F.; Scherf, U.; List, E. J. W.; Lanzani, G. *Phys. Rev. Lett.* **2008**, *100*, 57401.
(16) Virgili, T.; Cerullo, G.; Lüer, L.; Lanzani, G.; Gadermaier, C.; Bradley, D. D. C. *Phys. Rev. Lett.* **2003**, *90*, 247402.
(17) Dhoot, A. S.; Hogan, J. A.; Morteani, A. C.; Greenham, N. C. *Appl. Phys. Lett.* **2004**, *85*, 2256.
(18) Herz, L. M.; Phillips, R. T. *Phys. Rev. B* **2000**, *61*, 13691.
(19) Ariu, M.; Lidzey, D. C.; Sims, M.; Cadby, A. J.; Lane, P. A.; Bradley, D. D. C. *J. Phys.: Condens. Matter* **2002**, *14*, 9975.
(20) Khan, A. L. T.; Sreearunothai, P.; Herz, L. M.; Banach, M. J.; Köhler, A. *Phys. Rev. B* **2004**, *69*, 085201.
(21) Hayer, A.; Khan, A. L. T.; Friend, R. H.; Köhler, A. *Phys. Rev. B* **2005**, *71*, 241302.
(22) Dias, F. B.; Macanita, A. L.; Melo, J. S. de.; Burrows, H. D.; Güntner, R.; Scherf, U.; Monkman, A. P. *J. Chem. Phys.* **2003**, *118*, 7119.
(23) Grell, M.; Bradley, D. D. C.; Ungar, G.; Hill, J.; Whitehead, K. S. *Macromolecules* **1999**, *32*, 5810.
(24) Inbasekaran, M.; Wu, W.; Woo, E. P. US patent no. 5,777,070, 1998.
(25) Inbasekaran, M.; Woo E. P.; Wu, W. International Patent Application, WO99/20675, 1999.
(26) Kuehne, A. J. C.; Mackintosh, A. R.; Armstrong, D. R.; Pethrick, R. A. *Cent. Euro. J. Chem.* **2007**, *5*, 923.
(27) Jalviste, E.; Ohta, N. *J. Chem. Phys.* **2004**, *121*, 4730.
(28) Iimori, T.; Ara, A. M.; Yoshizawa, T.; Nakabayashi, T.; Ohta, N. *Chem. Phys. Lett.* **2005**, *402*, 206.
(29) Tsushima, M.; Ushizaka, T.; Ohta, N. *Rev. Sci. Instrum.* **2004**, *75*, 479.
(30) Cadby, A. J.; Lane, P. A.; Wohlgenannt, M.; An., C.; Vardeny, Z. V.; Bradley, D. D. C. *Synth. Met.* **2000**, *111*, 515.
(31) Grell, M.; Bradley, D. D. C.; Inbasekaran, M.; Ungar, G.; Whitehead, K. S.; Woo, E. P. *Synth. Mat.* **2000**, *111*, 579.
(32) Como, E. D.; Becker, K.; Feldmann, J.; Lupton, J. M. *Nano Lett.* **2007**, *7*, 2993.
(33) Becker, K.; Lupton, J. *J. Am. Chem. Soc.* **2005**, *127*, 7306.
(34) Tunno, T.; Caricato, A. P.; Caruso, M. E.; Luches, A.; Martino, M.; Romano, F.; Valerini, D.; Anni, M. *Appl. Surf. Sci.* **2007**, *253*, 6461.
(35) Endo, T.; Kobayashi, T.; Nagase, T.; Naito, H. *Jpn. J. Appl. Phys.* **2007**, *46*, L1093.
(36) Biagioni, P.; Celebrano, M.; Rossi, M. Z.; Poli, D. *Appl. Phys. Lett.* **2007**, *91*, 191118.
(37) Asada, K.; Takahashi, H.; Naito, H. *Thin. Sol. Films* **2006**, *509*, 202.
(38) Ariu, M.; Sims, M.; Rahn, M. D.; Hill, J.; Fox, A. M.; Lidzey, D. G.; Oda, M.; Gonzalez, J. C.; Bradley, D. D. C. *Phys. Rev. B* **2003**, *67*, 195333, and reference cited therein.
(39) Meskers, S. C. J.; Hubner, J.; Oestreich, M.; Bässler, H. *J. Phys. Chem. B* **2001**, *105*, 9139.
(40) Chunwaschirasiri, W.; Tanto, B.; Huber, D. L.; Winokur, M. J. *Phys. Rev. Lett.* **2005**, *94*, 107402.
(41) Liptay, W. In *Excited States*; Lim, E. C., Ed.; Academic Press: New York, 1974; Vol. 1, p 129.
(42) Bublit, G. U.; Boxer, S. G. *Annu. Rev. Phys. Chem.* **1997**, *48*, 213.
(43) Ohta, N. *Bull. Chem. Soc. Jpn.* **2002**, *75*, 1637.
(44) Jalviste, E.; Ohta, N. *J. Photochem. Photobiol. C: Photochem. Rev.* **2007**, *8*, 30.
(45) Ohta, N.; Kawabata, H.; Umeuchi, S.; Yamazaki, I. *Chem. Phys. Lett.* **1999**, *310*, 397.
(46) Emelianova, E. V.; van der Auweraer, M.; Bässler, H. *J. Chem. Phys.* **2008**, *128*, 224709.

JP9023052